

## Japanese encephalitis virus infects neural progenitor cells and decreases their proliferation

Sulagna Das and Anirban Basu

National Brain Research Centre, Manesar, Haryana, India

### Abstract

Japanese encephalitis virus (JEV), a common cause of encephalitis in humans, especially in children, leads to substantial neuronal injury. The survivors of JEV infection have severe cognitive impairment, motor and behavioral disorders. We hypothesize that depletion of neural progenitor cells (NPCs) by the virus culminates in neurological sequelae in survivors of Japanese encephalitis (JE). We utilized both *in vivo* model of JEV infection and *in vitro* neurosphere cultures to study progressive JEV infection. Cellular infection and cell death was determined by flow cytometry. BrdU administration in animals and in neurospheres was used to determine the proliferative ability of NPCs. JEV leads to massive loss of actively proliferating NPC population from

the subventricular zone (SVZ). The ability of JEV infected subventricular zone cells to form neurospheres is severely compromised. This can be attributed to JEV infection in NPCs, which however do not result in robust death of the resilient NPC cells. Instead, JEV suppresses the cycling ability of these cells, preventing their proliferation. JEV primarily targets at a critical postnatal age and severely diminishes the NPC pool in SVZ, thus impairing the process of recovery after the insult. This arrested growth and proliferation of NPCs might have an effect on the neurological consequences in JE survivors.

**Keywords:** cell cycle, Japanese encephalitis virus, neural progenitor cells, proliferation.

*J. Neurochem.* (2008) **106**, 1624–1636.

Flavivirus are important human pathogens causing variety of diseases ranging from mild febrile illness to severe encephalitis and haemorrhagic fever. Among them, *Japanese encephalitis virus* (JEV), a neurotropic one, is a major cause of acute encephalopathy (Diagana *et al.* 2007). The virus affects all age groups with highest incidence in children, having mortality rate of 25–40%. Approximately 3 billion people live in JEV endemic areas covering much of Asia with nearly 50 000 cases of JE reported each year. Of these, about 10 000 cases results in fatality and a high proportion (approximately one-third) of survivors have serious neurological and psychiatric sequelae (Kaur and Vрати 2003; Myint *et al.* 2007). The commonly encountered sequelae in JE survivors are mental retardation, learning disabilities, behavioral abnormalities, motor paralysis, speech and movement disorders (Gourie-Devi *et al.* 1995).

Children are particularly susceptible to neurotropic virus infections, and earlier studies of JEV infection in rats suggested that younger animals are more vulnerable to virus infection (Ogata *et al.* 1991). Moreover, a higher incidence of neurological sequelae is reported in children than in adults. In infants, the brain is still in a dynamic state of development, therefore infection to the brain at this time of development

can have devastating effects on mental functions later in life (Hagberg and Mallard 2005).

Neuronal death in JE results from both direct neuronal killing by the virus, as well as by a bystander method mediated by microglial activation and robust inflammatory attack (Ghoshal *et al.* 2007; Swarup *et al.* 2007). The central nervous system (CNS) responds to any neuronal loss by differentiating new neurons and astrocytes from resident populations of multipotential neural progenitors cells (NPCs) (Abrous *et al.* 2005). These NPCs reside in neurogenic areas of the brain such as the subventricular zone (SVZ) and the dentate gyrus of the hippocampus and have the potential to self-renew over a lifetime (Ming and Song 2005). It has been

Received April 21, 2008; revised manuscript received May 28, 2008; accepted May 30, 2008.

Address correspondence and reprint requests to Anirban Basu, National Brain Research Centre, Manesar, Haryana-122050, India. E-mail: anirban@nbrc.res.in

**Abbreviations used:** AnnV, Annexin V; CDK, cyclin-dependent kinase; DCX, Doublecortin; FACS, fluorescence activated cell sorter; FBS, fetal bovine serum; MEM, minimum essential medium; NPC, neural progenitor cell; PBS, phosphate-buffered saline; PFA, paraformaldehyde; PI, propidium iodide; SVZ, subventricular zone.

postulated in recent times that postnatal neurogenesis contributes to long-term synaptic plasticity as well as cognitive processes (Kokaia and Lindvall 2003). An insult to these NPCs would thus affect the recovery process of the brain following any insult and lead to long term deficits.

The regulation of NPC proliferation in response to various insults like infection and inflammation is being explored extensively in recent times (Das and Basu 2008). Infection of the NPCs by viruses seems to be primarily responsible for generation of the brain abnormalities and long-term cognitive deficits in a number of neurodevelopmental disorders. Recent studies have shown that Coxsackievirus, a common cause of enteroviral encephalitis in neonates, targets proliferating NPC pool in the neonatal CNS (Feuer *et al.* 2003, 2005). Cytomegalovirus, another leading cause of developmental disorder of CNS, preferentially infects the ventricular and subventricular zone and impairs the growth and proliferation of NPCs (Kosugi *et al.* 2000). Adult neurogenesis has been reported to be dysregulated by viral infection, like HIV, which inhibits proliferation of adult NPCs in hippocampus, thereby inducing dementia in HIV patients (Krahtwohl and Kaiser 2004; Okamoto *et al.* 2007).

Here, for the first time in the *Flaviviridae* family, we report that JEV can infect NPCs and harbor in them. Interestingly, the virus does not induce robust NPC death, but with progressive infection arrests their proliferative ability. This eventually culminates in depletion of NPC pool upon JEV infection, which could lead to long-term neurological sequel in JE survivors.

## Materials and methods

### Virus infection in animals

The GP78 strain of JEV was propagated in suckling BALB/c mice and their brains were harvested when symptoms of sickness were observed. A 10% tissue suspension was made in minimum essential medium (MEM), followed by centrifugation at 10 000 *g* to remove cellular debris and filtered through 0.22  $\mu$ m sterile filter. Virus was titrated by plaque formation using PS (porcine stable kidney) cell line (Vrati *et al.* 1999). Monolayers of PS cells were incubated with 10-fold dilutions of the virus made in MEM containing 1% fetal bovine serum (FBS) for 1 h at 37°C. After removing the viral inoculums, monolayers were overlaid with MEM containing 4% FBS, 1% low melting point agarose and a cocktail of antibiotic-antimycotic solution. Plates were incubated at 37°C for 3–7 days till plaques were visible. The plaques were then counted after fixing the cells with 10% formaldehyde and staining with crystal violet (Swarup *et al.* 2008).

Suckling BALB/c mice of either sex were injected intracerebrally with ~100 p.f.u [in 30  $\mu$ L of phosphate-buffered saline (PBS)] of virus, and control animals received the same amount of PBS. From third day post-infection (dpi), animals showed symptoms of JE including limb paralysis, poor pain response, and whole body tremor. On 4 dpi, all animals succumbed to infection. All experiments were performed according to protocols approved by Institutional Animal Ethics Committee.

### Neurosphere generation and virus infection of NPCs

Subventricular zone from BALB/c mouse pups (P7) were dissected out aseptically in (phosphate buffer with 1 mM MgCl<sub>2</sub> and 0.6% glucose) and minced mechanically. The tissue was then dissociated in a solution of 10 mg/mL Trypsin with 50  $\mu$ g/mL DNaseI at 37°C for 10 min and neutralized with Dulbecco's modified Eagle's medium containing 10% FBS. After centrifugation, the pellet was resuspended in Pro-N media (Dulbecco's modified Eagle's media/F12 containing 10 ng/mL D-biotin, 25  $\mu$ g/mL insulin, 6.29 ng/mL progesterone, 16.11  $\mu$ g/mL putrescine, 5 ng/mL selenium, 50  $\mu$ g/mL apo-transferrin, and 50  $\mu$ g/mL gentamycin). The suspension was passed through 40  $\mu$ m screen and then centrifuged at 300 *g* for 6 min. The cells were plated at density of  $3 \times 10^4$  cells/cm<sup>2</sup> in Pro-N media supplemented with 20 mg/mL epidermal growth factor and 10 mg/mL fibroblast growth factor (FGF; R&D Systems, Minneapolis, MN, USA). Fresh media was added after every 2 days.

The number of spheres and their diameter were measured after 7 days growth *in vitro* from control and JEV infected animals using Leica IM50 software. In all *in vitro* experiments, neurospheres were dissociated into single cell suspensions using Accutase and replated at lower density of  $3 \times 10^3$  cells/cm<sup>2</sup>. This plating at clonal density was for secondary neurosphere assays also. The secondary neurospheres were allowed to form for 7–8 days, following which number of spheres and diameter of spheres were determined. All other *in vitro* experiments were carried out after minimum two passages and under cell density of  $2 \times 10^4$  cells/cm<sup>2</sup> in 6 well plates.

The dissociated NPCs after 1.5 days in suspension were infected with JEV at MOI = 5 (Multiplicity of Infection), washed by centrifugation, and cultured with fresh Pro-N medium. At 1 day, 3 days and 7 days post-infection (dpi), samples were collected and counted by trypan blue exclusion. The NPCs were either processed for cell death or cell cycle assays using fluorescence activated cell sorter (FACS) or for immunoblot.

### Clonogenic assay

The primary neurospheres from SVZ of control and JEV infected animals after 7 days in culture were dissociated into single cell suspension as verified by hemocytometer. After counting cells, they were diluted and plated in 96-well plates at a density of single cell per well. Each of the wells was observed carefully under the microscope and those wells with single cells were marked. The total number of neurospheres in these wells after 10–12 days of growth was counted.

### Intracellular staining of JEV antigen by flow cytometry

The NPCs at different time points of JEV infection were dissociated using Accutase and washed twice in FACS buffer (PBS containing 3% serum and 0.09% sodium azide).  $1 \times 10^6$  cells were taken for each condition and they were fixed and permeabilized with Cytotfix/cytoperm buffer (BD Biosciences, CA, USA). After washing cells in FACS buffer, primary antibody (JEV Nakayama strain; Chemicon, Temecula, CA, USA) was added at 1 : 100 dilution in Perm/wash buffer for 1 h in ice. After washing thrice with Perm/Wash Buffer (BD Biosciences), secondary labeling was done with anti-mouse FITC (1 : 100, Vector Labs, Burlingame, CA, USA) for 30 min at 25°C. After three washes with Perm/wash buffer, samples were analyzed on FACS Calibur (Becton Dickinson) using Cell Quest Pro software. The percentage of antiJEV-FITC positive cells was

calculated after gating the populations ( $2 \times 10^4$  gated cells for each analysis) on Dot plot in Cell Quest Pro Software.

#### BrdU labeling and DNA content analysis

BALB/c mice pups from control and JEV infected groups (four animals in each group) received intraperitoneal injections of 5-bromo-2'-deoxyuridine (BrdU 50 mg/kg; Sigma) for 2.5 days, twice daily. These animals were sacrificed 6 h after the last injection and their brains were processed for immunohistochemistry. In another set of animals, a single BrdU pulse of 100 mg/kg body weight was given for 4 h. The SVZ was dissected out after 4 h in PGM buffer and single cell suspension was prepared.

*In vitro* labeling of NPCs with BrdU was done by treating NPCs with 20  $\mu$ M BrdU for 6 h, following which neurospheres were dissociated into single cell suspension using Accutase. Thereafter,  $1 \times 10^6$  cells were taken for each condition and proceeded for BrdU staining using BrdU Flow kit (BD Biosciences) according to the manufacturer's instructions. The BrdU positive cells were detected on FL-1 channel and the percentage of cells calculated using Dot plots in Cell Quest Pro software.

The analysis of cell cycle or DNA synthesis was performed by labeling cells with 7-AAD (BD Biosciences), a fluorescent dye that binds to DNA. The labeling with 7-AAD was done according to manufacturer's instructions in BrdU Flow kit. The labeled cells were detected on FL-3 channel by FACS and analyzed using Cell Quest Pro software to quantify the percentage of cells residing in different stages of cell cycle.  $1 \times 10^4$  gated cells were analyzed for each experimental condition.

#### Immunohistochemistry and immunocytochemistry

The brains from JEV infected animals and age matched controls were fixed in 4% paraformaldehyde (PFA) and cryoprotected. Fluorescence immunohistochemistry was performed on the 20 micron sections for the following antibodies: anti-Nakayama JEV (1 : 200, Chemicon), anti-JEV polyclonal antibody (1 : 100, a kind gift from Dr. Sudhanshu Vrat, National Institute of Immunology, New Delhi, India), anti-Nestin (1 : 250; Chemicon), anti-Ki67 (1 : 1000; Novocastra, Newcastle, UK), anti-BrdU (1 : 200; Sigma, St. Louis, MO, USA), anti-Doublecortin (DCX, 1 : 1000; Chemicon). Antigen retrieval using 0.1 M Citrate buffer (pH 6.0) was done for Ki67 and BrdU, followed by permeabilization with 6N HCl for 7 min at 25°C. The sections were then neutralized by washes with 0.1 M Borate buffer and blocked for 1 h in appropriate serum. All antibodies were incubated overnight at 4°C in a humid chamber. Respective secondary antibodies were used- FITC conjugated antibodies (1 : 200, Vector) and anti-mouse Alexa Fluor 594 (1 : 1000, Molecular Probes, Eugene, OR, USA).

The grown neurospheres were plated on Poly D-lysine coated chamber slides and allowed to adhere for 12 h. The spheres were fixed in 4% PFA for 20 min at 25°C, following which they were incubated in blocking solution for 1 h at 25°C. They were then stained for the markers of NPCs, Nestin (1 : 250) and Musashi (1 : 200, Chemicon), overnight at 4°C. After PBS washes, the corresponding FITC conjugated secondary antibodies were added (1 : 200, Vector) and then mounted with 4,6-diamidino-2-phenylindole (DAPI).

Terminal deoxynucleotidyl Transferase Biotin-dUTP Nick End Labeling (TUNEL) staining was also performed on control and JEV

infected NPCs at different dpi. After fixing cells in 4% PFA, the apoptotic cells were identified using *In situ* cell death detection kit, TMR Red (Roche, Germany) according to manufacturer's instructions. All slides were mounted with Vectashield with DAPI (Vector Labs) and visualized under Zeiss Apotome or under Zeiss Confocal microscope.

#### Cell death assay by Annexin-Propidium iodide staining

Uninfected control and JEV infected NPCs at different dpi were dissociated and collected in 1 $\times$  binding buffer (25 mM HEPES plus NaOH, pH 7.4, 140 mM NaCl and 1 mM CaCl<sub>2</sub>). Then, 100  $\mu$ L of each sample ( $1 \times 10^5$  cells) was incubated with 5  $\mu$ L each of FITC labeled Annexin V (AnnV) and propidium iodide (PI) (BD Biosciences) in dark for 15 min at 25°C. After adding 400  $\mu$ L of binding buffer in each tube, the samples were analysed by FACS Calibur using Cell Quest Pro Software.

#### Immunoblotting

Protein was isolated from control and JEV infected neurospheres using lysis buffer [1% Triton-X-100, 10 mM Tris-HCl (pH 8.0), 150 mM NaCl, 0.5% Nonidet P (NP-40), 1 mM EDTA, 0.2% EGTA, 0.2% sodium orthovanadate, and protease inhibitor cocktail] and quantified using Bradford Reagent (Ghoshal *et al.* 2007). 40 micrograms of protein was electrophoresed on polyacrylamide gel and transferred onto nitrocellulose membrane. The membranes were then blocked with 4% skimmed milk in PBS-Tween 20 (PBS-T) for 1 h and then incubated with the following antibodies: p21 (1 : 1000; Santa Cruz Biotechnology, Santa Cruz, CA, USA), p27 and cyclin D (1 : 2000; Abcam, Cambridge, UK). All primary antibodies were prepared in PBS-T with 1% bovine serum albumin, and incubated overnight with gentle agitation. After extensive washes with PBS-T, corresponding horse radish peroxidase conjugated secondary antibodies (1 : 2500, Vector Labs) prepared in PBS-T were added for 1 h. Blots were rinsed again in PBS-T and chemiluminescence reagent (Millipore, Bedford, MA, USA) was then added. The blots were developed by exposing in Chemigenius Bioimaging System (Syngene, UK) using GeneSnap software and the images were analyzed using GeneTools software provided with the same bioimaging system. The blots were stripped and reprobbed with anti- $\beta$ -tubulin (1 : 1000; Santa Cruz Biotechnology) as internal control.

#### RNA isolation and semi-quantitative RT-PCR

Brain tissue from control and JEV infected mice were homogenised in Trizol reagent (Sigma) and total cellular RNA was isolated according to previous protocols (Basu *et al.* 2002). Isolated RNA was quantified by spectrophotometry and reverse-transcribed using one-step RT-PCR kit (Qiagen Biosciences, Hamburg, Germany). One microgram of total RNA was used in a 25  $\mu$ L PCR reaction containing 5 $\times$  PCR buffer (5  $\mu$ L), dNTPs (1  $\mu$ L), Enzyme mix (1  $\mu$ L), specific forward and reverse primers (0.6  $\mu$ M) and RNase free water. Oligonucleotide primers for Nestin and Cyclophilin (internal control) were manufactured from Sigma (Bangalore, India) and produced single bands of predicted size (Supplementary Table S1). The PCR products were separated on 2% agarose gels, stained with ethidium bromide and photographed using Chemigenius Bioimaging System. Densitometric analysis of the bands was performed with Gene Tools software.

**Statistical analysis**

Results from all the experiments were analysed for statistical significance using paired and unpaired two-tailed Student's *t*-test.

**Results**

**Topographical distribution of JEV antigen in the virus infected brain**

Japanese encephalitis virus, a neurotropic virus targets the CNS and we wanted to determine the distribution of the viral antigen in different brain regions. Immunohistochemistry for anti-Nakayama JEV antibody showed that the viral antigen is expressed in all the brain areas primarily, cortex, striatum, hippocampus and SVZ (Fig. 1a–d). However, a qualitative examination revealed that the striatum and the SVZ have relatively high viral load compared to the cortex.

Double immunohistochemistry for Nestin and JEV antibody was performed on JEV infected sections, and indeed co-localisation of JEV and Nestin was observed (Fig. 1e). This clearly reflects that NPCs *in vivo* harbors the JE virus. The Nestin positive cells in the JEV infected brain show two kinds of morphology-oval-shaped cells which are JEV infected (Fig. 1e), and those with round cell bodies and processes where no colocalisation with the viral antigen was observed (Fig. 1f). These findings reveal that perhaps upon JEV infection the Nestin positive cells undergo some morphological changes and lose their cell processes.

**JEV decreases the NPC pool and their proliferative ability *in vivo***

We first evaluated the effect of JEV infection on SVZ, the primary neurogenic region of the brain. Immunohistochemistry for Nestin, a marker for NPCs demonstrated a dramatic

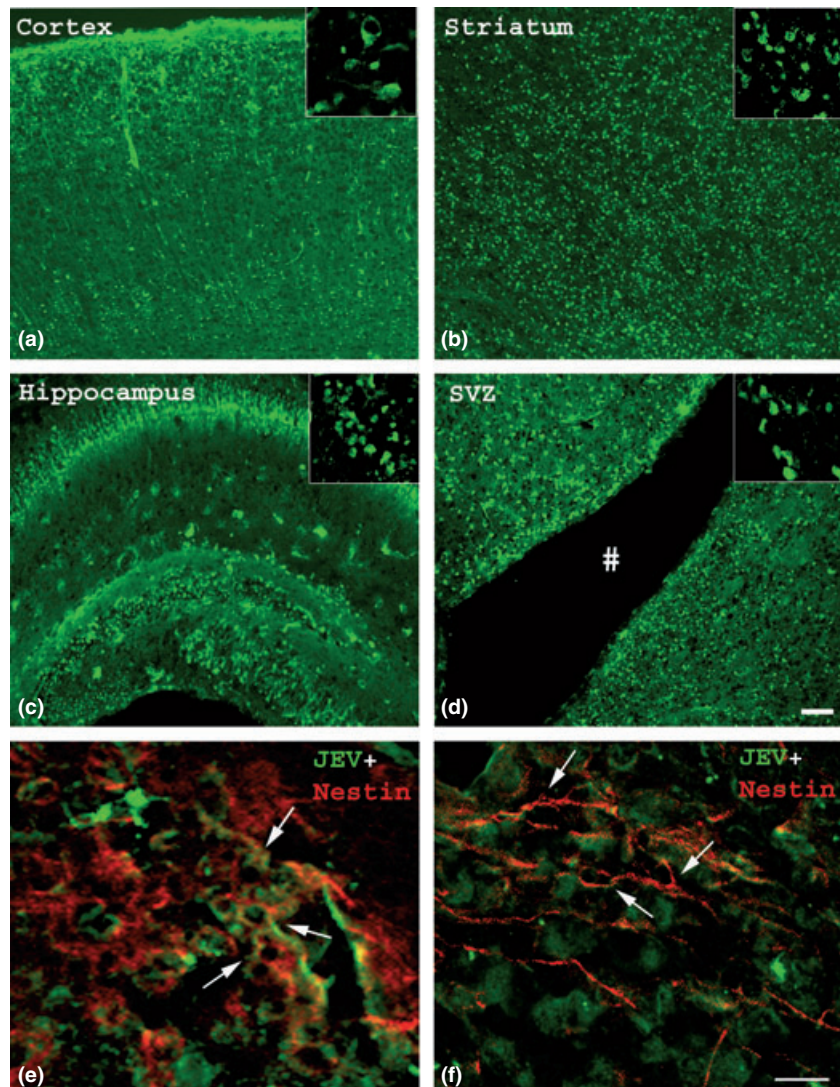


**Fig. 1** Distribution of JEV antigen in the brain and co-localisation with NPCs in the SVZ. Cryostat sections from JEV infected BALB/c mouse pups were processed for anti-Nakayama JEV antibody. A prominent expression of JEV antigen in different brain regions like cortex (a), striatum (b), hippocampus (c) and SVZ (d) was observed. The inset depicts a high magnification (40 ×) confocal image of the JEV infected cells in the corresponding areas. Scale bar corresponds to 100 microns. # indicates the lateral ventricle. Double immunohistochemistry was performed on JEV infected brain sections for anti-JEV polyclonal antibody (FITC, green) and anti-Nestin antibody (Alexa Fluor 594, red). Colocalisation of JEV antigen with the Nestin positive cells (e) has been indicated by white arrows, thus confirming the infection of NPCs by JEV *in vivo*. However, uninfected Nestin positive cells were also observed in the same JEV infected section (f), indicated by white arrows, with morphological characteristics different from JEV infected NPCs. Scale bar corresponds to 25 microns.

decrease in Nestin positive population in JEV infected SVZ as compared to age matched controls (Fig. 2a). This was further validated by semi-quantitative RT-PCR for Nestin, indicating a 2.5 fold reduction in Nestin mRNA in JEV infected brain than control ones (Fig. 2b) ( $p < 0.05$ ). The effect of JEV on NPC proliferation was next explored, and Ki-67 staining (Chenn and Walsh 2002) was performed. JEV infection indeed lowered the percentage of Ki-67 positive

cells by almost 2-fold below control in SVZ (Fig. 2c and d), as counted from five serial sections in three animals using Leica IM50 software. BrdU incorporation in the cells of SVZ helped to further determine the proliferative potential of NPCs. To clearly indicate that these proliferating cells were of the neuronal lineage, double staining for BrdU and DCX (a marker for migrating neuroblasts) was done. Upon JEV infection, the percentage of BrdU and DCX double positive

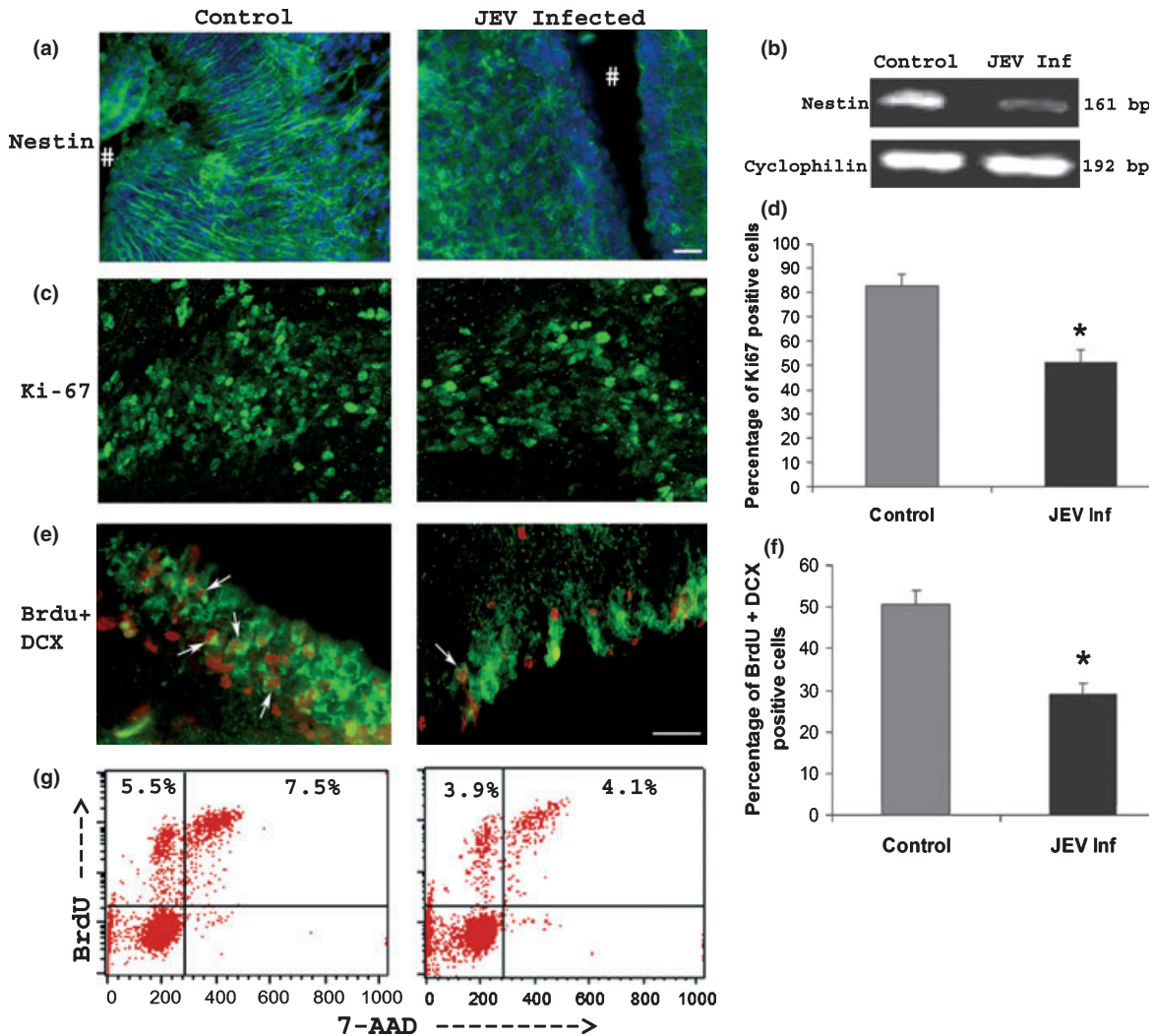


**Fig. 2** JEV infection *in vivo* causes loss of actively proliferating NPC population from SVZ. BALB/c mouse pups were either JEV infected or PBS injected and sacrificed after 4 days. BrdU was administered intraperitoneally for 2.5 days at 50 mg/kg body weight. Cryostat sections were stained for Nestin (a), Ki-67 (c) and doubled stained for BrdU and DCX (e). In another set of animals, single BrdU pulse (100 mg/kg body weight) for 6 h was given, and SVZ was dissected out from these animals. Single cell suspensions of control and JEV infected SVZ was BrdU labeled and detected by flow cytometry (g). A marked decrease in the Nestin positive cells (FITC, green) was observed in JEV infected SVZ than control SVZ (a). Semi-quantitative RT-PCR was performed to quantify Nestin expression, where, a significant decrease in JEV

infected brain was noticed compared to control brain (b). The proliferating cells indicated by Ki-67 staining (FITC, green) (c) and by BrdU (Alexa Fluor 594, red) - DCX (FITC, green) double staining (e) were also significantly reduced in JEV infected SVZ. Scale bar corresponds to 25 microns. # indicates the lateral ventricle. The graphs represent the percentage of Ki-67 and double positive BrdU + DCX cells as counted from five fields (d, f). Values represent mean  $\pm$  SEM from three independent experiments. \* Significant change from control  $p < 0.05$ . Quantitation of BrdU was done by FACS, by detecting the BrdU positive cells on FL-1 channel. A significant decrement in BrdU count was found in cells from JEV infected SVZ than control SVZ as analyzed by Cell Quest Pro software ( $p < 0.05$ ) (g).

cells were significantly reduced by almost 2-folds compared to that in control SVZ (Fig. 2e and f).

An exact quantification of the number of proliferating cells in the SVZ was determined by performing the BrdU count using flow cytometry. After a single pulse of BrdU (100 mg/kg body weight), the cells from SVZ were isolated and BrdU positive cells were detected by FACS. A significant decrease in BrdU positive cells from  $13 \pm 1.3\%$  in control SVZ to  $8 \pm 1.05\%$  in SVZ of JEV infected animals was observed (Fig. 2g) ( $p < 0.05$ ). All these observations summarize that JEV infection indeed diminishes the actively proliferating population of NPCs in the SVZ.

### JEV decreases the number of colony-forming neurospheres and their self-renewal capacity

The clonal neurosphere assay is an important assay that quantifies the number of NPCs in the SVZ and their self-renewal potency (Felling *et al.* 2006). A neurosphere is defined as a free-floating aggregate of minimum eight cells, though majority of the spheres are larger than this. The SVZ from control and JEV infected animals were microdissected and the single cell suspension ( $3 \times 10^4$  cells/cm<sup>2</sup> for both conditions) was cultured in presence of epidermal growth factor and fibroblast growth factor to form primary neurospheres. NPCs of JEV infected animals formed four times less spheres ( $6 \pm 1$ ) than those of control animals ( $23 \pm 3$ ) (Fig. 3a and b) ( $p < 0.05$ ). Moreover, neurospheres of JEV infected animals were noticeably smaller in diameter ( $120 \pm 17$  microns) than those of control animals ( $250 \pm 24$  microns) (Fig. 3c and d) ( $p < 0.05$ ).

One of the characteristic features of stem cells is their ability to self-renew, tested by secondary neurosphere assays (Reynolds and Weiss 1996). The primary neurospheres were dissociated and plated at very low densities (clonal densities) to assess the number of secondary spheres formed after 7 days in culture. The ability of the primary spheres from JEV infected animals to form secondary neurospheres was severely compromised, whereas the control primary spheres generated 6-fold more secondary spheres (Fig. 3e) ( $p < 0.05$ ).

Besides the secondary neurosphere assay, another method to accurately reflect the self-renewal potency is single-cell analysis in 96-well plate (Levison *et al.* 2003; Singec *et al.* 2006). In this assay each sphere is considered to have been generated from a single cell. The dissociated NPCs were plated at single cell per well in 96-well plates and spheres were counted after 10 days. 17% of the NPCs from control SVZ, had regenerated as spheres (Fig. 3f), whereas it decreased to 5% in case of NPCs from JEV infected SVZ. Thus, a 3-fold decrease in the sphere-generation ability from single cells was observed in NPCs from JEV infected SVZ than those from control SVZ ( $p < 0.05$ ). These results clearly indicate that the JEV infection abrogates the self-renewal capacity of NPCs.

### JEV infects NPCs and inhibits their growth with progressive infection

The neurospheres generated were characterized by performing immunocytochemistry for the markers of NPCs, Nestin and Musashi, both of which were robustly expressed by the neurospheres (Fig. 4a).

The dissociated NPCs were infected with JEV at a multiplicity of infection 5 (MOI = 5) and the time course of viral antigen expression on NPCs was determined by intracellular virus (anti-Nakayama JEV antibody) staining at different time points (3 h and 24 h) (Fig. 4b). While at 3 h only a few cells (2%) stained for JEV antigen, the number increased to 40% at 24 h post-infection. This indicated that the virus enters into NPCs *in vitro* and harbors in them.

The growth kinetics of NPCs was monitored over time course of viral infection. The cells were plated at a density of  $2 \times 10^4$  cells/cm<sup>2</sup> and after infection cell counting was performed. At 1 dpi there was no difference in the morphology and number of spheres between JEV infected and control NPCs. However, at 3 dpi, the diameter and the number of colony forming spheres showed significant reduction in JEV infected NPCs than uninfected controls. With progressive infection, at 7 dpi, the sphere count after JEV infection was reduced by 2 fold than control ( $p < 0.05$ ) (Fig. 4c and d). Moreover, average diameter of these spheres was markedly decreased from  $130 \pm 17$  microns in uninfected controls to  $85 \pm 14$  microns in JEV infected ones at 7 dpi (Fig. 4c and e) ( $p < 0.05$ ). In conjunction, these results indicated the permissiveness of the NPCs to JEV infection *in vitro* and the resulting aberrant formation of neurospheres with progressive infection.

### Effect of JEV infection on survivability of NPCs

Since JEV leads to massive neuronal loss (Mishra and Basu 2008), hence we investigated whether the diminished NPC population is due to JEV induced cell death. The apoptotic population was detected by TUNEL assay. Surprisingly, JEV infection at MOI5 (which yields 80% TUNEL positive cells in neurons) (Swarup *et al.* 2007) resulted in only 14% TUNEL positive cells in NPCs at 1 dpi. The percentage of TUNEL positive cells after JEV infection increased to 18% at 3 dpi, significantly higher than uninfected control ( $p < 0.05$ ), which however at 7 dpi was similar to control NPCs (Fig. 5a and b).

Cell death was also evaluated by flow cytometry of Annexin V-Propidium Iodide stained NPCs. Ann V versus PI dot plot which reveals four populations: living cells (AnnV-negative and PI-negative), living cells with a disturbed membrane (AnnV-negative and PI-positive), early apoptosis (AnnV-positive and PI-negative) and late apoptosis or necrosis (AnnV-positive and PI-positive) (van Genderen *et al.* 2006). Late apoptotic or necrotic cell death in JEV infected NPCs at 1 dpi was 7% versus 2.5% in control NPCs, which, however at 3 dpi increased to 11% compared to 2% in

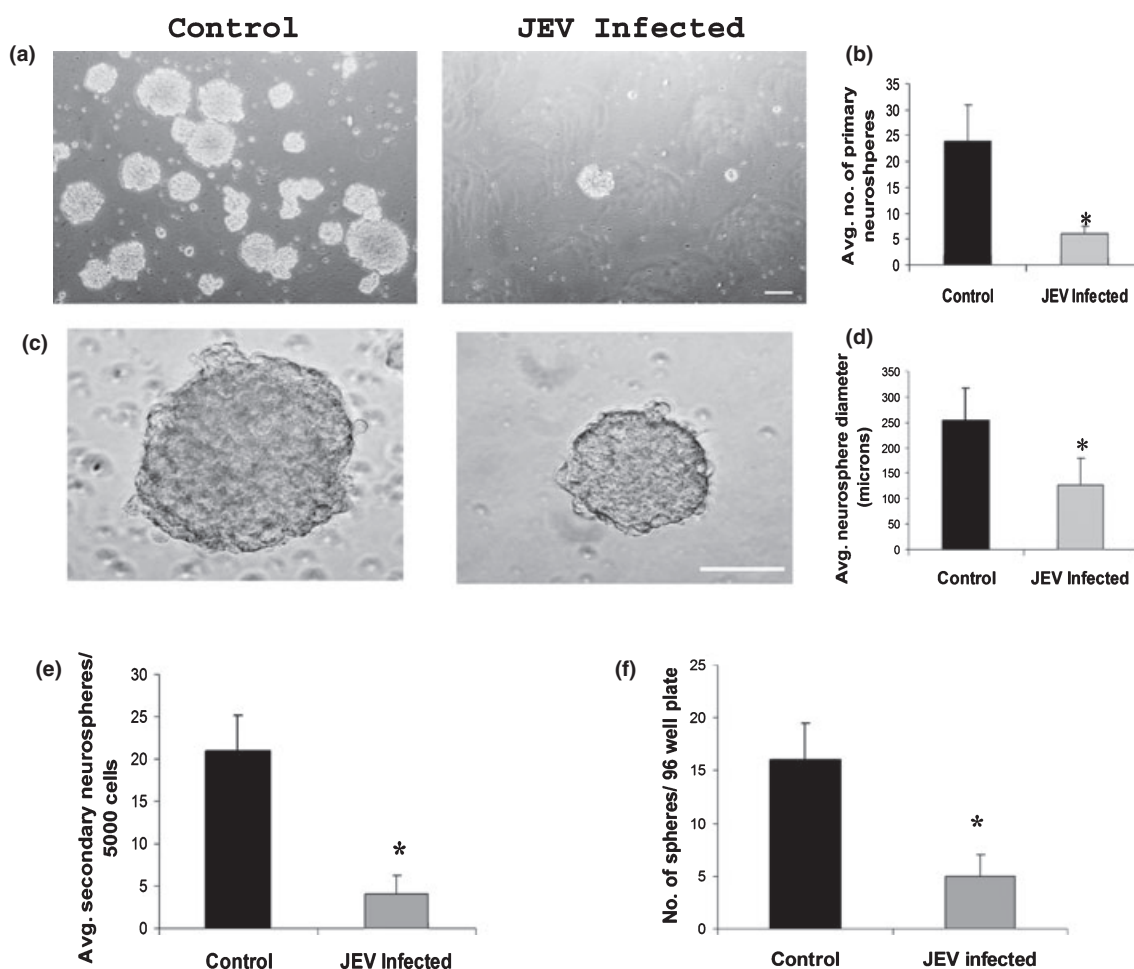


**Fig. 3** *In vivo* JEV infection reduces the number of colony forming NPCs and their self-renewal capacity. SVZ from JEV infected and age matched control animals were dissected out and dissociated into single cell suspension. The cells were then cultured in presence of FGF-2 (10 ng/mL) and EGF (20 ng/mL). Each experiment consisted of six pups in each group. The average number of primary neurospheres and their average diameter after 7 days in culture from control and JEV infected SVZ were compared. Neurospheres isolated from JEV infected animals were distinctively lesser in number than those from control SVZ ( $p < 0.05$ ) (a, b). Scale bar corresponds to 100 microns. Neurosphere size (as measured from 10 spheres in each condition) was markedly smaller in JEV infected SVZ (c). The

control NPCs ( $p < 0.05$ ) (Fig. 5c). At 7 dpi, this late apoptotic or necrotic population in JEV infected NPCs was comparable to uninfected controls. The results clearly suggest that though JEV induces cell death in NPCs to a certain extent, however it is not the primary factor dictating the reduction in NPC population following infection.

#### JEV infection inhibits DNA synthesis and cell cycle progression in NPCs

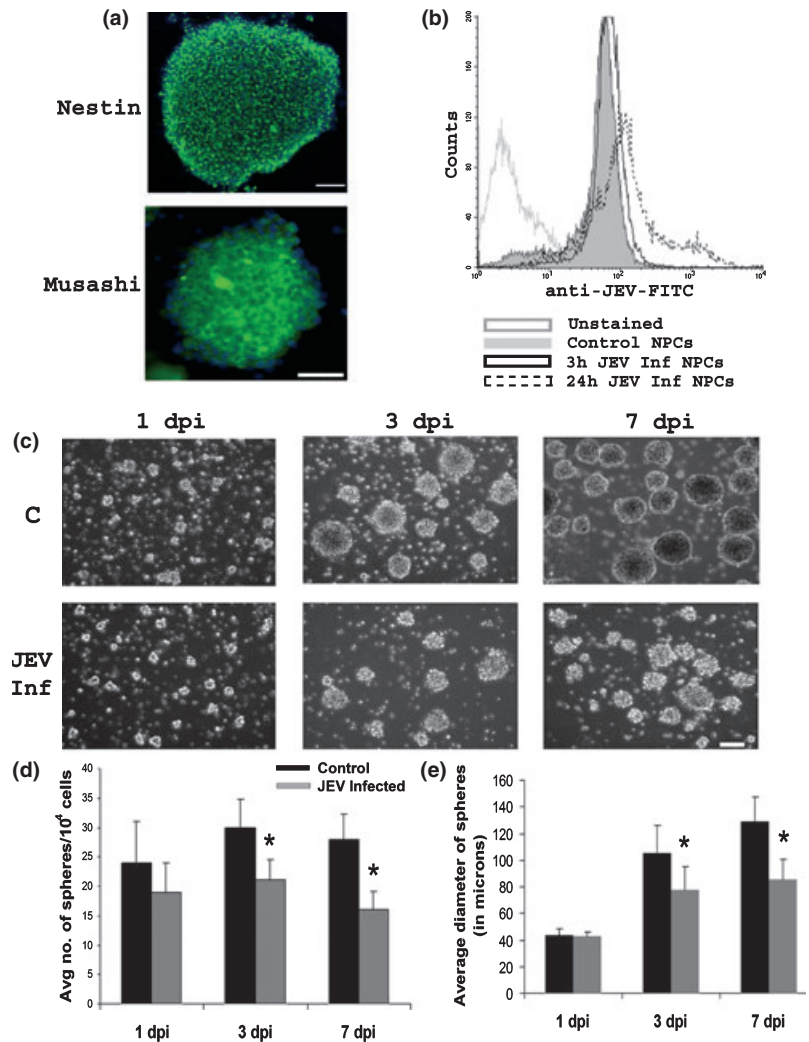
To address whether JEV mediated growth inhibition in NPCs results from attenuated proliferative ability or impaired DNA

graph represents the average diameter of the spheres in microns,  $p < 0.05$  (d). These primary neurospheres from control and JEV infected SVZ were then dissociated and subcultured at clonal densities to determine self-renewal rates of each condition. The graph represents the impaired ability of JEV infected primary NPCs to form secondary neurospheres (e). Clonogenic assay was also performed by plating single cells in 96-well plates. The wells with single cell per well were observed and after 10 days the numbers of spheres were counted. A significant decrease in the number of spheres generated from NPCs of JEV infected SVZ was observed (f). Values represent mean  $\pm$  SEM from four independent experiments. \* Significant change from control  $p < 0.05$ .

synthesis, BrdU incorporation experiments were performed. *In vitro*, at 1 dpi, no significant change in BrdU label was noticed, which however, at 3 dpi, reduced drastically from 20.9% in uninfected control to 7% in JEV infected NPCs. This 3-fold decrease in BrdU positive cells upon infection was seen in 7 dpi also (Fig. 6a). Reduced cumulative S-phase labeling in JEV infected NPCs thus clearly indicates that JEV inhibits the synthesis of DNA in NPCs.

Cell cycle kinetics in NPCs was analyzed by labeling with 7-AAD (Schmid *et al.* 2000), a fluorescent DNA binding dye. According to their DNA content, the NPCs were detected as

**Fig. 4** JEV infects NPCs *in vitro* and retards their growth. The mouse neurospheres were stained for markers of NPCs, Nestin and Musashi (a), both FITC labeled and merged with DAPI. Scale bar corresponds to 100 microns. Single cell suspensions of NPCs after 1.5 days in culture were infected with JEV (MOI = 5) for 1 h at 37°C and then replated in fresh media. At 3 h and 24 h post-infection, the uninfected and JEV infected NPCs were stained for anti-Nakayama JEV antibody. The FITC labeled cells were detected by Flow cytometry on FL-1 channel. While only a few NPCs stained positive for JEV antigen at 3 h, a significant population of JEV-FITC positive cells were observed at 24 h post-infection (b). The control and JEV infected NPCs were grown for different dpi and the number and size of the spheres were measured as mentioned before (c). Scale bar is 100 microns. The representative graph indicates the significant decrease in the number of colony forming neurospheres with progressive infection ( $p < 0.05$ ) (d). The reduction in size of JEV infected NPCs with respect to control NPCs was prominent at 3 and 7 dpi as indicated by the graph depicting the average size of the spheres ( $p < 0.05$ ) (e). Thus the self-renewal capacity of NPCs was noticeably impaired following JEV infection. \* Significant change from control NPCs,  $p < 0.05$ .



three different population on FL-3 channel-cells in G0/G1 (2n DNA), S (> 2n) and G2/M (4n) stages of cell cycle, with most of the cells residing in G0/G1 phase of cell cycle (Morrison *et al.* 1997). Interestingly, the number of cells residing in S-phase in JEV infected NPCs showed no significant difference from control NPCs at 1 dpi, which, however, at 3 dpi showed a 50% reduction (Fig. 6b). At 7 dpi also, this decrease in S-phase cells upon JEV infection was prominent and was 45% lower than uninfected NPCs (Supplementary Table S2). These findings were absolutely in correlation to the BrdU incorporation assays and strongly suggest that JEV infection indeed blocks cell cycle progression through S-phase in NPCs.

**JEV leads to up-regulation of G1->S phase checkpoint proteins**

We then investigated whether JEV modulates the various check-points proteins that are involved in cell cycle progression, especially in G1->S phase transition. Indeed, we found that p27 levels was upregulated by almost 3 fold in JEV infected NPCs at 3 dpi and 7 dpi than control NPCs. Similar

increase in p21 levels was also observed in JEV infected samples (Fig. 7a and c). Cyclin D expression is critical in the transition of cells from G1->S phase of cell cycle. A 4 fold decrease in level of cyclin D was noted in JEV infected NPCs at 3 dpi and a more pronounced 7 fold reduction at 7 dpi than uninfected controls (Fig. 7a and b). These results suggest that JEV by enhancing the expression of these checkpoint inhibitors leads to G1 phase arrest in the NPCs eventually resulting in suppression of their proliferation.

**Discussion**

In the present study we have shown that JEV, which infects and kills neurons, also depletes the neural progenitor pool with progressive infection. We report for the first time in the family of *Flaviviridae* that NPCs are permissive to JEV infection both *in vivo* and *in vitro*, which leads to their growth retardation. The pathophysiological relevance of these observations was supported by profound decrement in actively proliferating NPCs in the SVZ of JEV infected

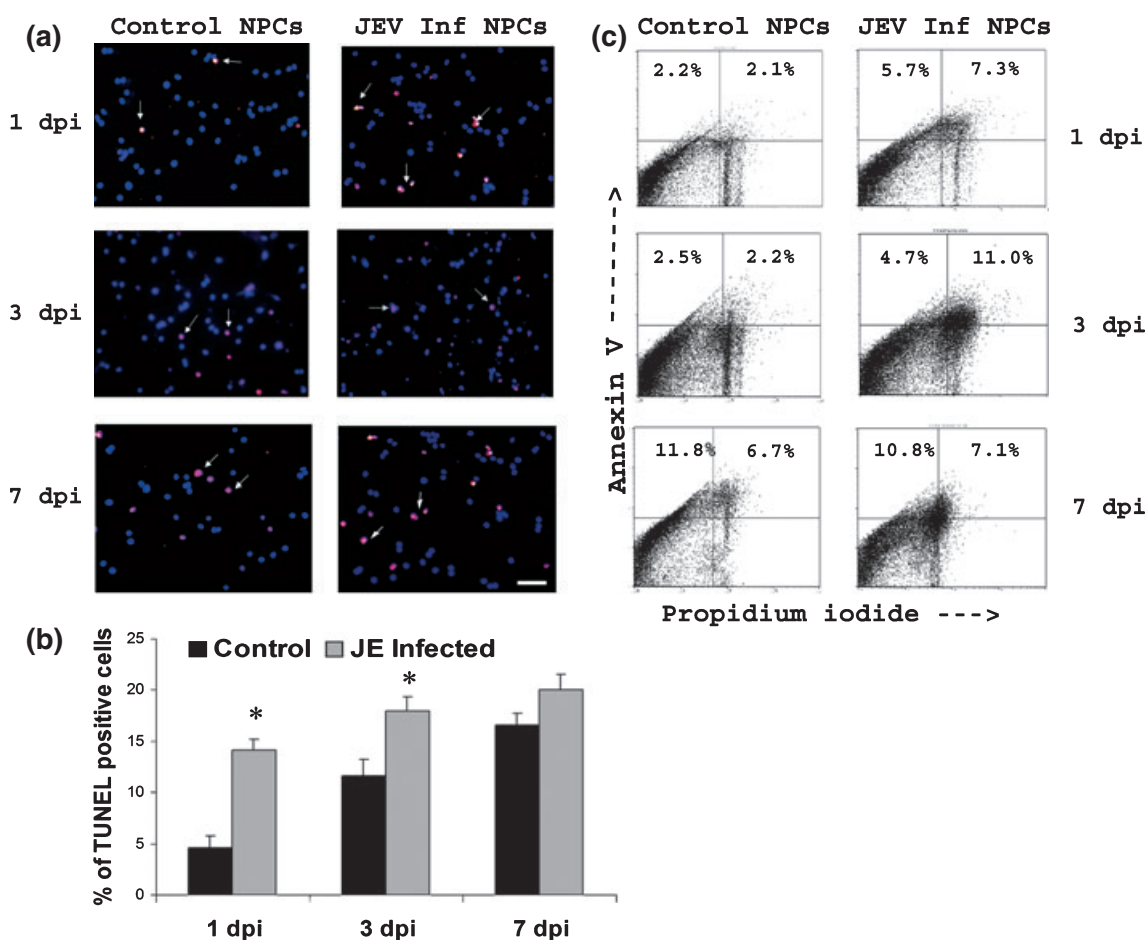


**Fig. 5** JEV infection and cell death in NPCs. Apoptotic cell death in control and JEV infected NPCs at different dpi was indicated by TUNEL positive cells (TMR-Red) colocalised with DAPI (shown by white arrows) (a). Scale bar is 25 microns. The number of TUNEL positive cells in JEV infected NPCs was higher than uninfected controls at 1 dpi and 3 dpi. At 7 dpi, the number of TUNEL positive cells in JEV infected was comparable to control NPCs. The graph represents the percentage of TUNEL positive NPCs cultured in control and JEV infected condition at different dpi (b). Values represent mean  $\pm$  SEM from three independent experiments performed in duplicates. \* Significant change from control NPCs,  $p < 0.05$ . Annexin V- Propidium iodide (Ann V-PI) staining was also performed on control and JEV

infected NPCs under similar dpi. Living cells are Ann V negative and PI negative, early apoptotic cells are Ann V positive but PI negative, whereas necrotic cells are both Ann V and PI positive. The percentage of cells which stained for Ann V and double stained for Ann V and PI are shown in the dot plots (c). One representative plot out of three experiments is shown. While a 2 fold increase in Ann V positive cells were noticed at 1 dpi and 3 dpi in JEV infected NPCs than control NPCs, however at 7 dpi no such increase was observed. Moreover, Ann-PI double positive cells also increased significantly in JEV infected NPCs than control ones by 2 fold and 4 fold at 1 dpi and 3 dpi respectively ( $p < 0.05$ ).

animals. Interestingly, the primary neurogenic area, SVZ has high viral load and the JEV infected Nestin positive cells in this region undergoes morphological alterations and impairment in proliferation ability. These findings suggest that infection of the NPCs and suppression of their proliferation might be primarily responsible for dysregulated neurogenesis in survivors of JE and development of cognitive deficits in them.

Neurogenesis continues beyond embryonic life and post-natal and adult neurogenesis has been postulated to have critical roles in learning, memory and cognitive development (Abrous *et al.* 2005; Lledo *et al.* 2006). In recent

years, it has been possible to study neurogenesis *in vitro* using the neurospheres as a model for proliferating multipotential NPCs (Reynolds and Weiss 1992, 1996). Neurotropic viruses like HIV disturb normal adult neurogenesis pattern, a possible cause for development of dementia in HIV patients. More importantly, it has been demonstrated that HIV infects the NPCs and leads to quiescence in these cells (Lawrence *et al.* 2004; Krathwohl and Kaiser 2004). Other neurotropic virus like Cytomegalovirus which targets the developing CNS also infects embryonic NPCs and replicates in them, inhibiting their growth and differentiation (Kosugi *et al.* 2000). Closely resembling these findings,

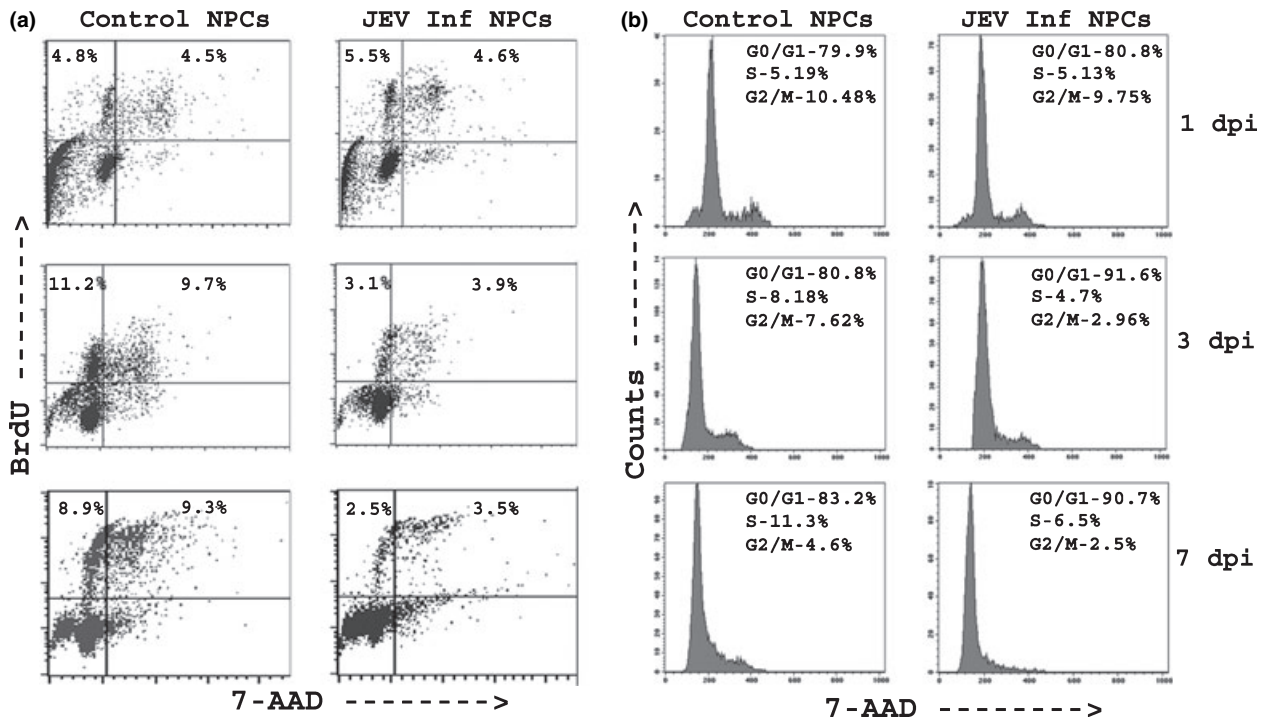


**Fig. 6** JEV inhibits proliferation and cell cycle progression in NPCs. Control and JEV infected NPCs were pulsed with 20  $\mu$ M BrdU for 6 h, then stained for BrdU and detected on FL-1 channel in FACS. The percentage of BrdU positive cells (both 2n and 4n DNA content state) have been indicated (a). A significant decrease in BrdU positive cells upon JEV infection was observed at 3 dpi and 7 dpi. The total percentage of BrdU labeled cells underwent a remarkable 3 fold reduction in JEV infected NPCs than control NPCs ( $p < 0.05$ ). One representative experiment out of three is shown. The different stages of cell cycle were evaluated using 7-AAD, a fluorescent DNA binding dye and

detected on FL-3 channel of FACS. Gates were set to assess the percentages of G0/G1 (2n DNA), S (> 2n DNA) and G2/M (4n DNA) cells using Cell Quest Pro Software. The percentages of cells in different stages of the cycle have been indicated in the representative histograms (b) and also in Supplementary Table S2. At 3 dpi and 7 dpi, the percentage of S-phase cells were decreased by 50% in JEV infected NPCs than in control NPCs, whereas those in G0/G1 phase were increased simultaneously ( $p < 0.05$ ). Moreover, the percentage of cells in G2/M phase also showed a gradual decrement with progressive infection.

we also report that JEV infects NPCs and expression of the viral antigen increases in these cells with time course of infection.

An outcome of JEV infection in NPCs is a decrease in their cell number, observed both *in vivo* in SVZ as well *in vitro* in neurosphere cultures. The decrement in NPC number can result from two phenomena- (i) cell death due to lytic infection or (ii) inhibition of cell proliferation due to blockade of cell cycle progression. Extensive neuronal loss is a feature of JEV-associated neurotropism (Yasui 2002) and mouse embryonic stem cell-derived neurons and neuroblastoma cells rapidly undergo apoptosis within 2–3 days after JEV infection (Yang *et al.* 2004). Besides JEV, several Flavivirus family members trigger apoptosis as part of the lytic infection, thereby helping in the dissemination of viral progeny.

Since JEV infects NPCs, we therefore determined the viral tropism in these cells and their susceptibility to JEV infection. By determining the apoptotic and necrotic population, we found that JEV induced cell death in NPCs

significantly increased at initial time points of infection, at 1 dpi and 3 dpi. However with progressive infection, cell death was comparable to that in control NPCs, thereby indicating that though virus induced lytic cell death occurs, however it does not contribute solely to the lowering of the NPC pool upon JEV infection. The initial necrotic death perhaps result from the endoplasmic reticulum stress that JEV induces initially, which then stabilizes at later time points (Su *et al.* 2002). These findings, though quite surprising, was supported by evidence indicating that HIV/gp120 even at effective concentration failed to induce cell death in NPCs (Okamoto *et al.* 2007). Interestingly, our results also showed that cell death observed in NPCs upon infection was significantly less compared to the extensive neuronal death in JEV. This can be explained by the findings in recent years which highlight that NPCs are a resilient population which has the potential to survive even in highly unfavorable conditions (Ricci-Vitiani *et al.* 2007).

Sustained proliferation is a key feature of NPCs and it has been recently shown that certain viruses like HIV and

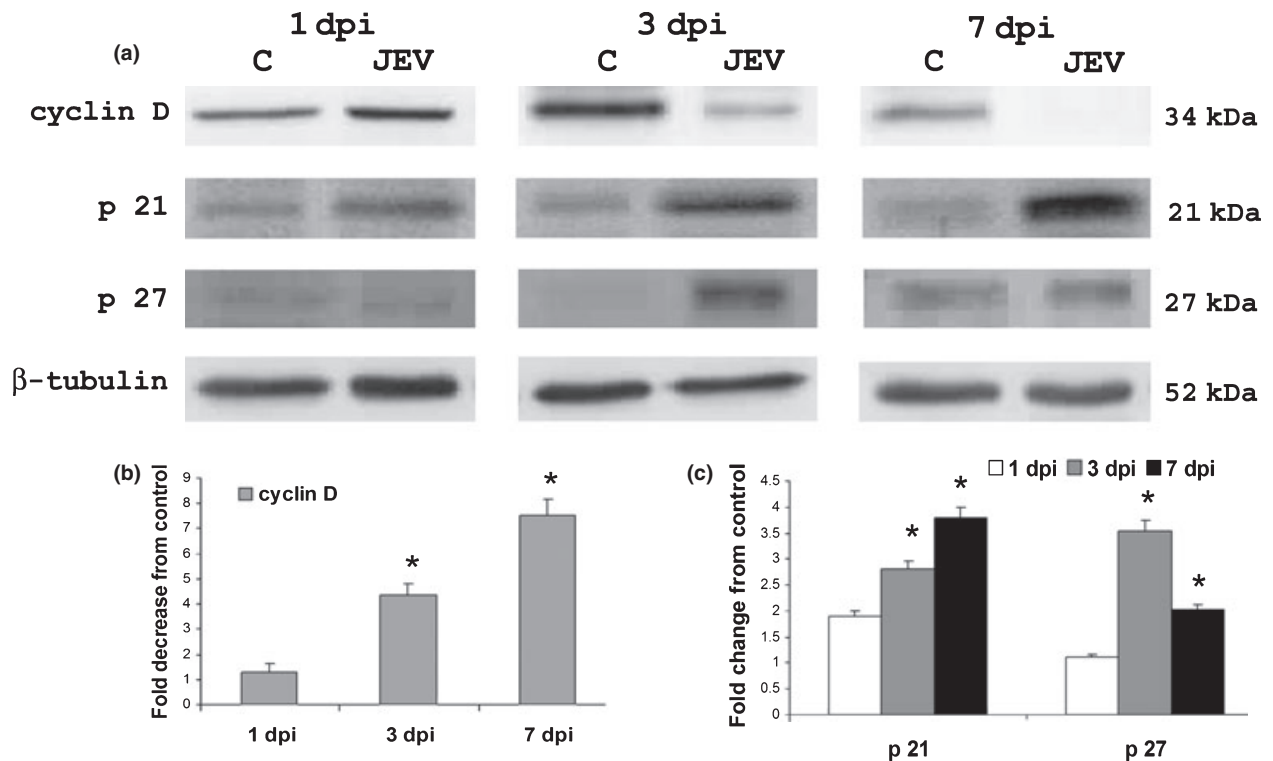


**Fig. 7** JEV arrests the G1->S phase progression by elevating the expression of checkpoint proteins. Protein was isolated from control and JEV infected NPCs at different dpi and immunoblotted for cyclin D, p21 and p27. While the levels of cyclin D was similar in both control and JEV infected NPCs at 1 dpi, its expression at 3 dpi and 7 dpi was drastically reduced in JEV infected samples (a, b). A significant ele-

vation in the expression of p21 and p27 was observed at 3 dpi and 7 dpi in JEV infected samples than control ones, indicating the arrest in G1->S phase transition of JEV infected NPCs (a, c). Densitometric analysis of immunoblot plotted as a bar graph (b, c). Values represent mean  $\pm$  SEM from three independent experiments. \*Significant change from control  $p < 0.05$ .

CMV can either induce quiescence in these cells by impairing their proliferative ability (Kosugi *et al.* 2000; Krathwohl and Kaiser 2004). In consistence to these reports, we also observed reduced Ki67 positive and BrdU + DCX double positive cells in JEV infected SVZ. Decreased incorporation of BrdU into NPCs both *in vivo* and *in vitro* suggested that JEV inhibits DNA synthesis in these NPCs during progressive infection. The decrement in DCX positive cell population and in DCX mRNA expression also has implications in the regulation of differentiation of these NPCs into neuronal lineages by JEV (Das and Basu, unpublished observations). Further validation of proliferation arrest in NPCs with progressive infection was obtained from cell cycle analysis, which clearly depicted that JEV indeed blocks S-phase entry with a very low percentage of cells residing in S-phase of the cycle. This observation emphasized cell cycle arrest as a possible mechanism of diminishing the NPC pool following infection. Cell cycle withdrawal and induction of G1 arrest via p38-MAPkinase pathway has also been reported as the mechanism by which HIV/gp120 suppresses proliferation of NPCs (Okamoto *et al.* 2007).

Cell cycle progression in NPCs is critically regulated and various cyclins and cyclin-dependent kinases (CDKs) orchestrate this process (Yoshikawa 2000). The progression through G1->S is initiated by cyclin D/CDK4(CDK6) complex and microinjections of cyclin D1 antisense plasmids prevents entry into S-phase (Baldin *et al.* 1993). Besides cyclins and CDKs, certain CDK inhibitors like p21 and p27 have been implicated in the progression through the G1 phase (Johnson and Walker 1999). These inhibitors block the transit through restriction point and thus force the cells to exit the cycle (Caviness *et al.* 1999). Based on these studies, enhanced expression of p21 and p27 and corresponding reduced levels of cyclin D in NPCs specifically indicated that JEV influences the G1->S phase transition. G1-phase arrest in NPCs and their slow cycling provides possible explanation for diminished NPC pool observed following JEV infection. In concordance to these results, previous reports indicate that HIV also induces G1 phase arrest and elevated p21 and p27 levels have been implicated in the NPCs (Krathwohl and Kaiser 2004).

This study, for the first time, describes a connection between NPC proliferation and the development of long term

cognitive deficits observed in almost one-third of JE survivors. Future work on the dynamics of viral replication in neurogenic areas in models of chronic and persistent JEV infection would provide further insights into the neuropathogenesis of the viral encephalitis.

## Acknowledgements

This work was supported by grant awarded to AB from the Department of Biotechnology, Award # BT/PR8682/Med/14/1273/2007. S.D. is a recipient of Senior Research Fellowship from University Grants Commission. We thank Prof. Vijayalakshmi Ravindranath, Director, National Brain Research Center for her continuous support and encouragement. The authors thank Dr Ellora Sen for her critical feedback in this work, and Kanhaiya Lal Kumawat for technical assistance. We also thank Dr. Soumya Iyengar and her lab members for their help in immunohistochemical techniques.

## Supplementary material

The following supplementary material is available for this article:

**Table S1** Primers used for RT-PCR experiments and expected size of amplified products.

**Table S2** Percentage of cells in different stages of cell cycle.

This material is available as part of the online article from: <http://www.blackwell-synergy.com/doi/abs/10.1111/j.1471-4159.2008.05511.x> (This link will take you to the article abstract).

Please note: Blackwell Publishing is not responsible for the content or functionality of any supplementary materials supplied by the authors. Any queries (other than missing material) should be directed to the corresponding author for the article.

## References

- Abrous D. N., Koehl M. and Le Moal M. (2005) Adult neurogenesis: from precursors to network and physiology. *Physiol. Rev.* **85**, 523–569.
- Baldin V., Lukas J., Marcote M. J., Pagano M. and Draetta G. (1993) Cyclin D1 is a nuclear protein required for cell cycle progression in G1. *Genes Dev.* **7**, 812–821.
- Basu A., Krady J. K., O'Malley M., Styren S. D., DeKosky S. T. and Levison S. W. (2002) The type 1 interleukin-1 receptor is essential for the efficient activation of microglia and the induction of multiple proinflammatory mediators in response to brain injury. *J. Neurosci.* **22**, 6071–6082.
- Caviness V. S. Jr, Takahashi T. and Nowakowski R. S. (1999) The G1 restriction point as critical regulator of neocortical neurogenesis. *Neurochem. Res.* **24**, 497–506.
- Chenn A. and Walsh C. A. (2002) Regulation of cerebral cortical size by control of cell cycle exit in neural precursors. *Science* **297**, 365–369.
- Das S. and Basu A. (2008) Inflammation: a new candidate in modulating adult neurogenesis. *J. Neurosci. Res.* **86**, 1199–1208.
- Diagana M., Preux P. M. and Dumas M. (2007) Japanese encephalitis revisited. *J. Neurol. Sci.* **262**, 165–170.
- Felling R. J., Snyder M. J., Romanko M. J., Rothstein R. P., Ziegler A. N., Yang Z., Givogri M. I., Bongarzone E. R. and Levison S. W. (2006) Neural stem/progenitor cells participate in the regenerative response to perinatal hypoxia/ischemia. *J. Neurosci.* **26**, 4359–4369.
- Feuer R., Mena I., Pagarigan R. R., Harkins S., Hassett D. E. and Whitton J. L. (2003) Coxsackievirus B3 and the neonatal CNS: the roles of stem cells, developing neurons, and apoptosis in infection, viral dissemination, and disease. *Am. J. Pathol.* **163**, 1379–1393.
- Feuer R., Pagarigan R. R., Harkins S., Liu F., Hunziker I. P. and Whitton J. L. (2005) Coxsackievirus targets proliferating neuronal progenitor cells in the neonatal CNS. *J. Neurosci.* **25**, 2434–2444.
- van Genderen H., Kenis H., Lux P., Ungeth L., Maassen C., Deckers N., Narula J., Hofstra L. and Reutelingsperger C. (2006) In vitro measurement of cell death with the annexin A5 affinity assay. *Nat. Protoc.* **1**, 363–367.
- Ghoshal A., Das S., Ghosh S., Mishra M. K., Sharma V., Koli P., Sen E. and Basu A. (2007) Proinflammatory mediators released by activated microglia induces neuronal death in Japanese encephalitis. *Glia* **55**, 483–496.
- Gourie-Devi M., Ravi V. and Shankar S. K. (1995) Japanese Encephalitis: an overview. *Recent Advances in Tropical Neurology* 217–235.
- Hagberg H. and Mallard C. (2005) Effect of inflammation on central nervous system development and vulnerability. *Curr. Opin. Neurol.* **18**, 117–123.
- Johnson D. G. and Walker C. L. (1999) Cyclins and cell cycle checkpoints. *Annu. Rev. Pharmacol. Toxicol.* **39**, 295–312.
- Kaur R. and Vrati S. (2003) Development of a recombinant vaccine against Japanese encephalitis. *J. Neurovirol.* **9**, 421–431.
- Kokaia Z. and Lindvall O. (2003) Neurogenesis after ischaemic brain insults. *Curr. Opin. Neurobiol.* **13**, 127–132.
- Kosugi I., Shinmura Y., Kawasaki H., Arai Y., Li R. Y., Baba S. and Tsutsui Y. (2000) Cytomegalovirus infection of the central nervous system stem cells from mouse embryo: a model for developmental brain disorders induced by cytomegalovirus. *Lab. Invest.* **80**, 1373–1383.
- Krathwohl M. D. and Kaiser J. L. (2004) HIV-1 promotes quiescence in human neural progenitor cells. *J. Infect. Dis.* **190**, 216–226.
- Lawrence D. M., Durham L. C., Schwartz L., Seth P., Maric D. and Major E. O. (2004) Human immunodeficiency virus type 1 infection of human brain-derived progenitor cells. *J. Virol.* **78**, 7319–7328.
- Levison S. W., Druckman S. K., Young G. M. and Basu A. (2003) Neural stem cells in the subventricular zone are a source of astrocytes and oligodendrocytes, but not microglia. *Dev. Neurosci.* **25**, 184–196.
- Lledo P. M., Alonso M. and Grubb M. S. (2006) Adult neurogenesis and functional plasticity in neuronal circuits. *Nat. Rev. Neurosci.* **7**, 179–193.
- Ming G. L. and Song H. (2005) Adult neurogenesis in the mammalian central nervous system. *Annu. Rev. Neurosci.* **28**, 223–250.
- Mishra M. K. and Basu A. (2008) Minocycline neuroprotects, reduces microglial activation, inhibits caspase 3 induction, and viral replication following Japanese encephalitis. *J. Neurochem.* **105**, 1582–1595.
- Morrison S. J., Shah N. M. and Anderson D. J. (1997) Regulatory mechanisms in stem cell biology. *Cell* **88**, 287–298.
- Myint K. S., Gibbons R. V., Perng G. C. and Solomon T. (2007) Unravelling the neuropathogenesis of Japanese encephalitis. *Trans. R. Soc. Trop. Med. Hyg.* **101**, 955–956.
- Ogata A., Nagashima K., Hall W. W., Ichikawa M., Kimura-Kuroda J. and Yasui K. (1991) Japanese encephalitis virus neurotropism is dependent on the degree of neuronal maturity. *J. Virol.* **65**, 880–886.
- Okamoto S., Kang Y.-J., Brechtel C. W., Siviglia E., Russo R., Clemente A., Harrop A., McKercher S., Kaul M. and Lipton S. W. (2007) HIV/gp120 decreases adult neural progenitor cell proliferation via

- checkpoint kinase-mediated cell- cycle withdrawal and G1 arrest. *Cell Stem Cell* **1**, 230–236.
- Reynolds B. A. and Weiss S. (1992) Generation of neurons and astrocytes from isolated cells of the adult mammalian central nervous system. *Science* **255**, 1707–1710.
- Reynolds B. A. and Weiss S. (1996) Clonal and population analyses demonstrate that an EGF-responsive mammalian embryonic CNS precursor is a stem cell. *Dev. Biol.* **175**, 1–13.
- Ricci-Vitiani L., Lombardi D. G., Signore M., Biffoni M., Pallini R., Parati E., Peschle C. and De Maria R. (2007) Human neural progenitor cells display limited cytotoxicity and increased oligodendrogenesis during inflammation. *Cell Death Differ.* **14**, 876–878.
- Schmid I., Cole S. W., Korin Y. D., Zack J. A. and Giorgi J. V. (2000) Detection of cell cycle subcompartments by flow cytometric estimation of DNA-RNA content in combination with dual-color immunofluorescence. *Cytometry* **39**, 108–116.
- Singec I., Knoth R., Meyer R. P., Maciaczyk J., Volk B., Nikkhah G., Frotscher M. and Snyder E. Y. (2006) Defining the actual sensitivity and specificity of the neurosphere assay in stem cell biology. *Nat. Methods* **3**, 801–806.
- Su H. L., Liao C. L. and Lin Y. L. (2002) Japanese encephalitis virus infection initiates endoplasmic reticulum stress and an unfolded protein response. *J. Virol.* **76**, 4162–4171.
- Swarup V., Das S., Ghosh S. and Basu A. (2007) Tumor necrosis factor receptor-1-induced neuronal death by TRADD contributes to the pathogenesis of Japanese encephalitis. *J. Neurochem.* **103**, 771–783.
- Swarup V., Ghosh J., Mishra M. K. and Basu A. (2008) Novel strategy for treatment of Japanese encephalitis using arctigenin, a plant lignan. *J. Antimicrob. Chemother.* **61**, 679–688.
- Vrati S., Agarwal V., Malik P., Wani S. A. and Saini M. (1999) Molecular characterization of an Indian isolate of Japanese encephalitis virus that shows an extended lag phase during growth. *J. Gen. Virol.* **80**(Pt 7), 1665–1671.
- Yang K. D., Yeh W. T., Chen R. F., Chuon H. L., Tsai H. P., Yao C. W. and Shaio M. F. (2004) A model to study neurotropism and persistency of Japanese encephalitis virus infection in human neuroblastoma cells and leukocytes. *J. Gen. Virol.* **85**, 635–642.
- Yasui K. (2002) Neuropathogenesis of Japanese encephalitis virus. *J. Neurovirol.* **8**(Suppl 2), 112–114.
- Yoshikawa K. (2000) Cell cycle regulators in neural stem cells and postmitotic neurons. *Neurosci. Res.* **37**, 1–14.